An Integrated Human–Cyber–Physical Framework for Control of Microgrids

Shuai Feng, *Member, IEEE*, Michele Cucuzzella, *Member, IEEE*, Thijs Bouman, Linda Steg, and Jacquelien M. A. Scherpen, *Fellow, IEEE*

***Abstract*—In this paper, to jointly study the energy dynamic behavior of humans and the corresponding physical dynamics of the microgrid, we bridge two disciplines: systems & control and environmental psychology. Firstly, we develop second order motivation-behavior mathematical models inspired by opinion dynamics models for describing and predicting human activities related to the use of energy, where psychological variables and social interactions are considered. Secondly, based on these models, we develop a human-cyber-physical system framework consisting of three layers: (i) human, (ii) cyber and (iii) physical. The first one describes human behavior influenced by behavioral intervention and motivation, which in turn depend on contextual factors, personal values and social norms. The cyber layer solves an optimization problem and embeds load controllers, which are designed to automatically mimic human behavior. Finally, the physical layer represents an AC microgrid. Thus, we formulate a social-physical welfare optimization problem and solve it by designing a distributed primal-dual control scheme, which generates the optimal behavioral intervention (with respect to a given reference) and the control inputs to the microgrid.**

***Index Terms*—Control and psychology, control of microgrids, optimization.**

I. Introduction

INDIVIDUALS' energy behavior can critically affect the functioning of energy systems. A good understanding of individuals' behavior and its drivers is needed to accurately model and optimize energy systems. Knowledge on such drivers in psychology could be employed to better understand individuals' energy behavior that affects the energy system's functioning, and to promote the behavior that makes the energy system function more optimal, possibly enhancing the effectiveness of technical solutions [1], [2].

In control and optimization problems for microgrids, modeling human behavior has attracted increasing attention. For instance, in [3], based on hidden Markov modeling techniques, the authors have built models capturing variations in consumer habits of daily life. When the consumer requests to activate a time-shiftable appliance, based on the model and control algorithm, the activation request will be accepted or postponed. The work in [4] proposes a model describing the load behavior of individual households using Markov chains, and then develops a control strategy for consumption reduction. In [5], the authors consider Demand Side Management (DSM) to optimize the energy consumption and, based on population dynamics, model the dynamic behavior of humans participating/quitting DSM programs. In [6], an incentive (price) based method is proposed to reduce the peaks of demand. In particular, through smart meters, the users can receive different pricing schemes for optimally managing flexibility.

To simultaneously analyse the energy dynamic behavior of humans and the physical dynamics of the microgrid, we present an interdisciplinary work that integrates systems & control and psychology. We first develop feasible mathematical models describing human activities related to the use of energy. Then, to model the impact of dynamical human behavior on a microgrid and the effects of behavioral interventions (e.g., financial incentives) on energy use, we develop a *human-cyber-physical system (HCPS)* framework, based on which we obtain the optimal inputs to the microgrid (e.g., to control inverters and controllable loads) as well as suitable behavioral interventions. Specifically, the HCPS includes three layers. The first one is the human layer, which describes human activities; the second one is the cyber layer and consists of an optimal control system; the third one is the physical layer, i.e., an islanded AC microgrid (see Figure 1).

Energy behavior in psychology: The dynamic human behavior models proposed in this paper are inspired by findings in psychology. It is well established that energy use behavior is rooted in an individual's *personal values* (values for short), which reflect general goals that people strive for in life [2]. Personal values typically influence an individual's energy behavior via *motivation*, indexing a person's willingness to perform a behavior [7].

This paper considers three types of values that appear particularly relevant to energy behavior: *egoistic values* that imply

Manuscript received 22 May 2022; revised 3 November 2022 and 19 January 2023; accepted 9 February 2023. Date of publication 22 February 2023; date of current version 23 August 2023. This work was supported in part by the Dutch Research Council (NWO); in part by the ERA-Net Smart Energy Systems; and in part by the European Union's Horizon 2020 Research and Innovation Program under Grant 775970. Paper no. TSG-00733-2022. *(Corresponding author: Michele Cucuzzella.)*

Shuai Feng is with the School of Automation, Nanjing University of Science and Technology, Nanjing 210014, China (e-mail: s.feng@njust.edu.cn).

Michele Cucuzzella is with the Department of Electrical, Computer and Biomedical Engineering, University of Pavia, 27100 Pavia, Italy (e-mail: michele.cucuzzella@unipv.it).

Thijs Bouman and Linda Steg are with the Faculty of Behavioural and Social Sciences, University of Groningen, 9712 TS Groningen, The Netherlands (e-mail: t.bouman@rug.nl; e.m.steg@rug.nl).

Jacquelien M. A. Scherpen is with the Jan C. Willems Center for Systems and Control, ENTEG, Faculty of Science and Engineering, University of Groningen, 9747 AG Groningen, The Netherlands (e-mail: j.m.a.scherpen@rug.nl).

Color versions of one or more figures in this article are available at https://doi.org/10.1109/TSG.2023.3247918.

Digital Object Identifier 10.1109/TSG.2023.3247918

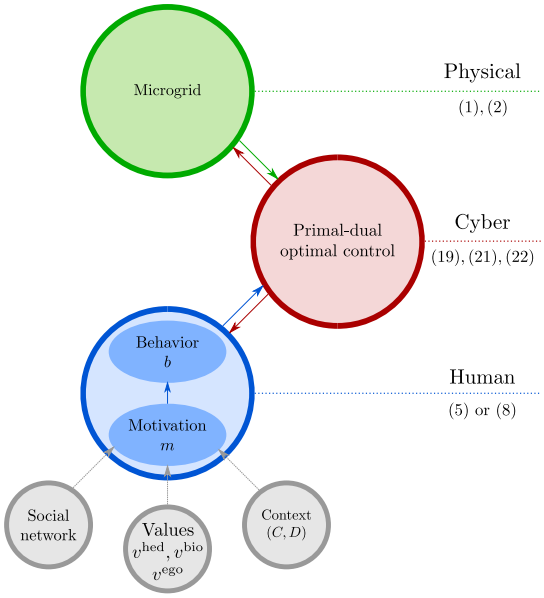

Fig. 1. Schematic representation of the proposed HCPS framework.

people aim to enhance their resources such as possessions, money and status, *hedonic values* that imply people aim to increase pleasure and comfort, and *biospheric values* that reflect a concern to protect nature and the environment [1], [8]. Stronger endorsement of biospheric values likely results in stronger motivation to save energy, which in turn increase the likelihood that someone will actually engage in energy saving behavior. Conversely, stronger endorsement of hedonic values is typically indicative of a weaker motivation to save energy because saving energy may be considered inconvenient or uncomfortable to do, which may demotivate energy saving behavior [9]. Individuals may also be motivated to increase/decrease their energy consumption because of associated behavioral intervention such as subsidies and taxes, which may particularly appeal to people who care relatively much about finances. Moreover, social influence can affect people's energy consumption. For instance, if an individual believes that most others regard saving energy the right thing to do (i.e., injunctive social norm) or see most others to engage in energy saving behaviour (i.e., descriptive social norm), this can motivate them to save energy as well [10], [11]. Also, we briefly discuss the effects of contextual factors on people's motivation and the resulting energy behavior [12].

HCPS framework: Energy behavior is influenced by the underlying motivation and behavioral intervention. From a control perspective, the behavioral intervention can be considered as a "control input" to the individual's behavior dynamics, while motivation can be considered as "reference signal" for the behavior in absence of behavioral intervention. On the other hand, from the viewpoint of opinion dynamics, motivation can be considered as the "opinion" concerning energy behavior of users which may affect others in a social network. For this reason, our models describing motivation are partially inspired by and consistent with studies in opinion dynamics [13], [14].

For the physical layer, we consider an islanded AC microgrid where people (prosumers) generate power within their local electricity facilities (e.g., PV panels, energy storage devices), which are connected through a distribution power network. The prosumers' loads are equipped with local control units that are designed to automatically mimic human behavior influenced by behavioral intervention. The local control units can also exchange necessary information, e.g., current generation, with their neighboring control units in the microgrid and are responsible for regulating the microgrid voltage towards a given value. Thus, the cyber layer (control system and communication network) acts as interface between the human and physical layers, guaranteeing the grid stability and adjusting automatically the loads by taking into account individuals' behavior.

We formulate a convex social-physical welfare optimization problem, whose solution corresponds to "control inputs" to the microgrid (i.e., voltage sources) and load control units (i.e., intervention). We aim at i) maximizing the social welfare by satisfying the prosumers' load demand and minimizing the cost associated to the behavioral intervention; ii) maximizing the physical welfare by guaranteeing grid stability and voltage regulation while minimizing the cost associated to current generation. To achieve these goals, we design a dynamic controller, whose unforced dynamics represent the primal-dual dynamics of the considered optimization problem [15], [16], [17]. The main contributions of this paper are:

- We bridge systems & control and psychology by developing a novel HCPS framework to study and analyze dynamic energy behavior of humans, taking into account the dynamics of the physical infrastructures of an islanded AC microgrid.
- To connect control and psychology, we develop models describing the dynamics of users' motivation and behavior studied in psychology, which are influenced by personal values, intervention and social norms.

To the best of our knowledge, such a framework incorporating psychology has never been developed and studied from a control perspective. Our work is partially inspired by [15], which studies a social-physical welfare optimization problem depending on prosumers' motives. More precisely, in [15] a DC microgird is considered, where however the prosumers dynamic behavior is neglected and hence no dynamic models describing energy consumption are used. In our paper, we deal with an AC microgrid as physical layer, which has more complex dynamics than a DC microgrid, and dynamic loads influenced by the dynamic behaviour of users. Moreover, in [15] the controller generates inputs only to the microgrid, while the proposed control framework generates also optimal behavioral intervention to affect users' energy consumption in a socially acceptable way. In [5], the behavior of human is modeled by two modes: joining or quitting DSM programs. Different from this binary type of switching model, we let the proposed control scheme reduce users' demand in a "continuous" fashion, and the degree of reduction depends on the motivation (i.e., personal values) of each user and the degree to which each user is influenced by interventions. Additionally, we develop also the control for the considered microgrid, which is not considered in [5].

TABLE I
PARAMETERS AND VARIABLES ($g \in \{d, q\}$)

Table of parameters		Table of variables	
L_{ti}	Filter inductance	I_{Lgi}	Load current
R_{ti}	Filter resistance	I_{tgi}	Generated current
L_k	Line inductance	V_{gi}	Load voltage
R_k	Line resistance	I_{gk}	Line current
C_{ti}	Filter capacitance	u_{gi}	Control input
R_{Li}	Load impedance	$b_i(u_{li})$	Behavior (load control)

Paper outline: This paper is organized as follows. In Section II, we develop the overall HCPS framework and introduce the so-called layer equation to deal with its slow-fast dynamics. In Section III we present the control objectives and in Section IV we design a primal-dual controller and analyze the closed-loop stability. A numerical example is presented in Section V, and finally Section VI ends the paper with some conclusions.

Notation: We denote by $\mathbb{R}$ the set of real numbers. Given $y \in \mathbb{R}$, $\mathbb{R}_{\geq y}$ denotes the set of reals no smaller than y. For any $w \in \mathbb{Z}$, we denote $\mathbb{Z}_{\geq w} := \{w, w+1, \ldots\}$. Let $\mathbf{0}$ and $\mathbf{1}$ denote column vectors of appropriate dimensions, having all 0 and 1 elements, respectively. Given a state $x \in \mathbb{R}^n$ with $n \in \mathbb{Z}_{\geq 1}$, we let $\bar{x}$ denote its steady state. Let $\mathbf{I}$ denote the identity matrix with appropriate dimension. Given a vector v, let $\|v\|$ denote its ℓ_2 norm. We let $\mathcal{N}$ denote the set of $N \in \mathbb{Z}_{\geq 2}$ prosumers and $\mathcal{E}$ denote the set of $E \in \mathbb{Z}_{\geq 1}$ transmission lines interconnecting the prosumers. Moreover, let $\mathcal{N}_i \subseteq \mathcal{N}$ denote the set of prosumers physically interconnected with prosumer i in the microgrid, and $\mathcal{E}_i \subseteq \mathcal{E}$ denote the set of the transmission lines connected to prosumer i. Let $\mathcal{S}_i \subseteq \mathcal{N}$ denote the set of the social neighbors of prosumer i.

II. HCPS FRAMEWORK

Before presenting the overall HCPS framework in Section II-C, we will first introduce the AC microgrid model in Section II-A, and then the human motivation-behavior models in Section II-B (see Figure 1).

A. AC Microgrid Model

We consider a low-voltage islanded AC microgrid composed of N prosumers that are connected by E resistive-inductive transmission lines. From a physical point of view, we assume that every prosumer can be represented by a Distributed Generation Unit (DGU), or equivalently a distributed storage unit, including a Voltage Sourced Converter (VSC) and a load (see Figure 2). We let $\omega_0 = 2\pi f_0$ be the speed of the rotating dq reference frame, where f_0 denotes the nominal frequency of the microgrid. Then, provided that the microgrid is balanced and symmetric, and all clocks of the internal oscillators are synchronized, we apply the Clarke's and Park's transformation to obtain the system dynamics in the rotating dq-frame [18], [19].

Given the notation in Table I, the (physical) dynamics of the of prosumer $i = 1, 2, \ldots, N$, can be expressed as

$$C_{ti}\dot{V}_{di} = \omega_0 C_{ti} V_{qi} + I_{tdi} + \sum_{k\in\mathcal{E}_i} I_{dk} - \frac{V_{di}}{R_{Li}} - I_{Ldi}u_{li} \quad (1a)$$

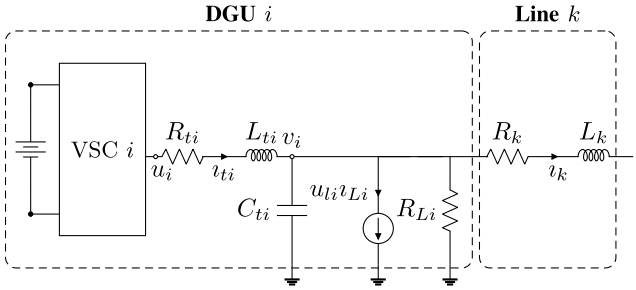

Fig. 2. Electrical single-line diagram of the DGU i and line k of a typical islanded AC microgrid, where v_i, $\imath_{ti}$, $\imath_k$, $\imath_{Li}$ and u_i are the three-phase electrical signals in the stationary abc-frame.

$$C_{ti}\dot{V}_{qi} = -\omega_0 C_{ti} V_{di} + I_{tqi} + \sum_{k\in\mathcal{E}_i} I_{qk} - \frac{V_{qi}}{R_{Li}} - I_{Lqi}u_{li} \quad (1b)$$

$$L_{ti}\dot{I}_{tdi} = -V_{di} - R_{ti}I_{tdi} + \omega_0 L_{ti} I_{tqi} + u_{di} \quad (1c)$$

$$L_{ti}\dot{I}_{tqi} = -V_{qi} - R_{ti}I_{tqi} - \omega_0 L_{ti} I_{tdi} + u_{qi}, \quad (1d)$$

where the d and q subscripts represent the direct and quadrature component, respectively. The resistance R_{Li} can represent the base load of prosumer i or simply the system's (parallel) damping, while $I_{Lgi}u_{li}$, $g \in \{d, q\}$, represent controllable current loads, i.e., loads equipped with local control units (e.g., smart home controllers). In particular, I_{Ldi} and I_{Lqi} are constants representing the nominal load currents of prosumer i, while $u_{li} : \mathbb{R} \to [0, 1]$ is the load control input that will be automatically adjusted by a suitable controller, whose dynamics depend on the model of human behavior, which will be introduced in the next subsection. For example, if $u_{li} = 0$ or $u_{li} = 1$ for all t, then the actual current absorbed by the loads of prosumer i is 0 or I_{Lgi}, respectively. Note that due to the dynamic load control input u_{li}, the current absorbed by the load of prosumer i, i.e., $I_{Lgi}u_{li}$, is generally time-varying. Moreover, in Section V, we will show simulation results where also the nominal load currents I_{Lgi} are time-varying and u_{li} can be greater than 1.

In (1), I_{dk} and I_{qk} denote the current exchanged between prosumers i and $j \in \mathcal{N}_i$ through the line $k \in \mathcal{E}_i$. The ends of the transmission line connecting prosumers i and j are arbitrarily labeled by "+" and "−". Then, the incidence matrix $\mathcal{B}$ for the "labeled" graph is given as $\mathcal{B}_{i,k} = +1$, if prosumer i is the positive end of the labeled transmission line $k \in \mathcal{E}_i$, $\mathcal{B}_{i,k} = -1$, if prosumer i is the negative end of the labeled transmission line $k \in \mathcal{E}_i$, otherwise, $\mathcal{B}_{i,k} = 0$. Suppose that prosumer i is the positive end of the transmission line k, then, the dynamics of I_{dk} and I_{qk} are given by

$$L_k\dot{I}_{dk} = V_{di} - V_{dj} - R_k I_{dk} + \omega_0 L_k I_{qk} \quad (2a)$$

$$L_k\dot{I}_{qk} = V_{qi} - V_{qj} - R_k I_{qk} - \omega_0 L_k I_{dk}. \quad (2b)$$

B. Human Motivation-Behavior Models

In this subsection, we focus on modeling human activities related to the consumption of energy. This will be beneficial for designing load controllers (e.g., smart home controllers and/or suitable Apps [20]) that automatically mimic human behavior. Specifically, we consider two different cases: **case i)** without social influence through descriptive norms

and **case ii)** with social influence through descriptive norms. Before presenting our models, we first provide in the following for the readers' convenience the definitions of personal values (egoistic, hedonic and biospheric), motivation, behavioral intervention, social norms and contextual factors.

Personal values reflect general and desirable life goals which are used as guiding principles in people's lives to evaluate actions and situations on. Research has identified a set of universal values, meaning every individual endorses these values to some extend. However, individuals differ in how strongly they endorse each value. The more an individual endorses and prioritizes a value, the more influential this value is for someone's preferences and actions [21], [22]. In case of energy behavior, three values appear of particular relevance:

- *Egoistic values* concern goals to acquire possessions, money and status. Energy behavior is often associated with financial benefits, which may motivate individuals with stronger egoistic values to engage in energy behavior for increasing/decreasing the consumption [9].
- *Hedonic values* concern striving for pleasure and comfort. Energy saving behavior may require effort or obstruct people from taking certain (convenient) actions, which is why energy saving behaviors may thwart hedonic values. Accordingly, people with stronger hedonic values are expected to have a weaker motivation to save energy.
- *Biospheric values* reflect goals to care about nature and the environment. Energy savings have clear environmental benefits, which is why stronger endorsement of biospheric values is typically indicative of stronger motivation, and thereby stronger engagement in energy saving behavior [23].

Motivation indexes a person's willingness to perform a behavior, e.g., the stronger an individual's motivation to save energy, the more likely this individual is to engage in energy saving behavior. Motivation is generally influenced by personal values. In the context of this paper, when someone strongly endorses biospheric and/or hedonic values, this individual is likely to experience a motivation to take the corresponding actions [24]. For instance, individuals who strongly endorse biospheric values typically feel a stronger motivation to take actions to save energy, eventually increasing the likelihood they will engage in energy saving behavior.

Behavioral intervention includes subsidies and financial rewards that can promote energy savings/consumptions by making it more attractive. The impact of financial incentives is likely more pronounced for individuals with stronger egoistic values, as such individuals care relatively much about money and possessions [9], [23]. Other examples of intervention are persuasion, social support and legal regulation [12].

Social norms in this paper represent the perception that others in a group/community intend to save energy. Social norms can motivate people to engage in sustainable energy saving behavior [10], particularly when the majority does engage in such behavior [11].

Contextual factors in this paper refer to situations that can decrease/increase behavioral 'cost', and hence motivate/demotivate people to act upon the corresponding values. For example, in some situations, pro-environmental actions (e.g., use less air conditioners in the summer) are generally associated with very high behavioural 'costs', e.g., convenience and comfort. As a result, people are less motivated to act upon biospheric values in those situations [25].

TABLE II
TABLE OF HUMAN DYNAMICS

Table of variables			
b_i	Behavior	$1/a_i$	Behavior time constant
m_i	Motivation	b_{ij}	Weight of social influence
s_i	Behavioral intervention	c_i	Weight of hedonic values
v_i^{hed}	Hedonic values	d_i	Weight of biospheric values
v_i^{bio}	Biospheric values	h_i	Weight of intervention
v_i^{ego}	Egoistic values		

Now, we present the proposed human models related to the use of energy.

Case i) For the dynamics of prosumer i, we propose the following second order dynamic system

$$\dot{b}_i = a_i(m_i - b_i - h_i s_i) \tag{3a}$$

$$\dot{m}_i = c_i\left(v_i^{\text{hed}} - m_i\right) + d_i\left(v_i^{\text{bio}} - m_i\right), \tag{3b}$$

where b_i and m_i are the states describing human behavior and motivation, respectively; and s_i is the "control input" of (3) representing behavioral intervention and it will be designed in Section IV (see (19) and (21)). All the other variables and parameters in (3) will be explained in the following (see also Table II). Also, we observe that for a given $\bar{s}_i$, the steady-state of system (3) satisfies

$$\bar{b}_i = \bar{m}_i - h_i\bar{s}_i \tag{4a}$$

$$\bar{m}_i = \left(c_i v_i^{\text{hed}} + d_i v_i^{\text{bio}}\right) \Big/ (c_i + d_i). \tag{4b}$$

Finally, the compact form of (3) can be written as

$$\dot{b} = A(m - b - Hs) \tag{5a}$$

$$\dot{m} = C\left(v^{\text{hed}} - m\right) + D\left(v^{\text{bio}} - m\right), \tag{5b}$$

where A, H, C and D are diagonal, e.g., $A = \text{diag}(a_1, \ldots, a_N)$.

We interconnect the human layer (3) and the physical layer (1), (2) through the cyber layer, i.e., through the design of an optimal primal-dual controller (see Sections III, IV and also Figure 1). Specifically, the human and physical layers are interconnected through the proposed behavior-based load control, i.e., $u_{li} = b_i$. Detailed explanations about the variables and parameters of system (3) are given in the following.

State and control variables:

a) b_i*:* By choosing $u_{li} = b_i$, this quantity represents the degree of supply of the load demand, with $0 \le \bar{b}_i \le 1$ for a non-negative s_i. For a negative s_i, b_i can be greater than 1, i.e., energy consumption is promoted by interventions, e.g., making charging plug-in electric vehicles cheaper when the microgrid overall generation/consumption is larger/smaller [26]. More precisely, it is the control input that automatically adjusts the current load demand $I_{Lgi}b_i$ of node i by mimicking the behavior of prosumer i. The closer b_i is to 1, the more satisfied the load demand of prosumer i is. This is a key variable that plays the role of interface between the physical layer (1), (2) and the human one (3).

b) m_i: Motivation, with $0 \le m_i \le 1$. From (3b), the solution m_i can be expressed as follows

$$m_i = e^{-(c_i+d_i)t}(m_i(0) - \bar{m}_i) + \bar{m}_i, \tag{6}$$

with $0 \le m_i(0) \le 1$ and $\bar{m}_i$ in (4b). If we omit in (3a) the term $-h_i s_i$ (see the following items for the meaning of h_i and s_i), m_i can be considered as a "reference signal" for the behavior b_i in absence of behavioral intervention ($s_i = 0$) or when behavioral intervention has no influence on prosumer i ($h_i = 0$). Thus, $h_i s_i = 0$ implies $b_i \to m_i$ when time approaches infinity. This essentially describes the phenomenon for which the motivation m_i acts as a guide for the behavior b_i.

c) s_i: Behavioral intervention, with $\bar{s}_i \le \bar{m}_i/h_i$. We require $\bar{s}_i \le \bar{m}_i/h_i$ since it prevents behavioral intervention from being unreasonably large at the steady state. The variable s_i is the "control input" to the behavior of prosumer i. Since h_i is non-negative (see the following items), $s_i \ge 0$ represents behavioral intervention that can motivate people to save energy and $s_i < 0$ for increasing energy consumption. For a given $\bar{s}_i$ and $\bar{m}_i$, it follows from (4a) that a larger value of $\bar{s}_i$ leads to a smaller value of $\bar{b}_i$. For instance, this can describe the phenomenon for which major behavioral intervention generally leads to more energy savings. From (3a) and (4a), one can observe that also motivation besides behavioral intervention influence individuals' energy behavior.

Constant parameters:

d) The item h_i indicates the degree of influence of behavioral intervention s_i on the energy behavior b_i. In particular, as mentioned above, in case of intervention corresponding to financial benefits, it is reasonable to consider $h_i = v_i^{\text{ego}}$, in which $0 \le v_i^{\text{ego}} \le 1$ represents egoistic values. Clearly, stronger egoistic values ($v_i^{\text{ego}} \to 1$) imply larger values of h_i. One can observe from (4a) that relatively large values of v_i^{ego} indicate that financial benefits can have stronger influence on motivating prosumer i to change energy consumption.

e) v_i^{hed}: hedonic values, with $0 \le v_i^{\text{hed}} \le 1$. The stronger the hedonic values are, the closer v_i^{hed} to 1 is, leading to higher energy consumption.

f) v_i^{bio}: Biospheric values, with $0 \le v_i^{\text{bio}} \le 1$. The stronger the biospheric values are, the closer v_i^{bio} to 0 is, leading to lower energy consumption.

g) $1/a_i > 0$ indicates the time constant of the behavior dynamics b_i. One can observe that a larger value of a_i implies a faster response of b_i to variations of m_i and s_i. Moreover, $c_i \ge 0$ and $d_i \ge 0$ such that $c_i + d_i > 0$ represent the weights of hedonic and biospheric values, respectively, indicating the degree to which each of these values influences the motivation of prosumer i. From (4b), one can observe that a relatively large value of c_i implies $\bar{m}_i \to v_i^{\text{hed}}$, i.e., prosumer i strongly endorses the hedonic values v_i^{hed}. On the other hand, a relatively large value of d_i implies $\bar{m}_i \to v_i^{\text{bio}}$.

Case ii) Differently from case i), now we consider also the influence of social norms, which may motivate people to engage in sustainable energy-saving behavior. Then, the dynamics in (3b) are replaced by

$$\dot{m}_i = \sum_{j \in \mathcal{S}_i} b_{ij}(m_j - m_i) + c_i\left(v_i^{\text{hed}} - m_i\right) + d_i\left(v_i^{\text{bio}} - m_i\right), \tag{7}$$

where m_j with $j \in \mathcal{S}_i$ denotes the motivation of the social neighbors of prosumer i, and $b_{ij} \in \mathbb{R}_{\ge 0}$ represents the weight of the social influence. Then, the compact model for the case including social norms is given by

$$\dot{b} = A(m - b - Hs) \tag{8a}$$

$$\dot{m} = C\left(v^{\text{hed}} - m\right) + D\left(v^{\text{bio}} - m\right) - \mathcal{L}m, \tag{8b}$$

where $\mathcal{L}$ is the Laplacian matrix associated with the social network, which in this paper is represented by an undirected connected graph. Note that the social network topology is not necessarily identical to the physical topology of the microgrid. For the sake of exposition, in the following sections we will mainly focus on case i). Then, we extend the results to case ii).

We assume all the parameters of systems (5) and (8) to be constant over the considered time windows. In order to capture the effect of changes in these parameters both on the transient and steady state, in Section V we will also show simulation results where some of these parameters change during the considered time window.

Remark 1: The proposed models are partially inspired by and consistent with some studies on opinion dynamics. First, they are partially consistent with some opinion dynamics models in which the "topics" (state variables) are possibly more than one and logically correlated [14]. Indeed, the proposed models have two correlated topics, i.e., b and m, with the topic m affecting the topic b. Second, the dynamics of m in (7) are also partially consistent with the continuous-time Friedkin-Johnsen model [13], where an individual is stubborn about his/her opinion m_i (depending on v^{hed} and v^{bio}) and may also be influenced by others' opinion.

C. HCPS Framework and Layer Equation

Recalling from the previous section that the physical layer (1), (2) and the human layer (5) (or (8)) are interconnected through the proposed behavior-based load control, i.e., $u_{li} = b_i$, we have

$$C_t\dot{V}_d = -R_L^{-1}V_d + \omega_0 C_t V_q + I_{td} + \mathcal{B}I_d - I_{Ld}b \tag{9a}$$

$$C_t\dot{V}_q = -\omega_0 C_t V_d - R_L^{-1}V_q + I_{tq} + \mathcal{B}I_q - I_{Lq}b \tag{9b}$$

$$L_t\dot{I}_{td} = -V_d - R_t I_{td} + \omega_0 L_t I_{tq} + u_d \tag{9c}$$

$$L_t\dot{I}_{tq} = -V_q - \omega_0 L_t I_{td} - R_t I_{tq} + u_q \tag{9d}$$

$$L\dot{I}_d = -\mathcal{B}^T V_d - RI_d + \omega_0 L I_q \tag{9e}$$

$$L\dot{I}_q = -\mathcal{B}^T V_q - \omega_0 L I_d - RI_q \tag{9f}$$

$$\dot{b} = A(m - b - Hs) \tag{9g}$$

$$\dot{m} = C\left(v^{\text{hed}} - m\right) + D\left(v^{\text{bio}} - m\right). \tag{9h}$$

Note that (9) is a slow-fast system in which (9a)–(9g) correspond to the fast dynamics and (9h) corresponds to the slow ones [27]. The time scales of them can be significantly different, e.g., the transient response of (9a)–(9g) can occur within some milliseconds or seconds, and the one of (9h) can be days, weeks or longer. Hence, the slow-fast system (9) can be decomposed into two simpler subsystems, the slow and the fast ones, which allow for a more thorough understanding of the interplay between the slow dynamics of the human

motivation, and the fast dynamics of the microgrid (including the behavior-based load control). In the context of our paper, we are interested in how human behaviour influences the microgrid (e.g., voltage, demand and current generation). Thus, it is reasonable to transform (9) into the so-called Layer Equation, which allows us to inspect the fast dynamics [28]. In a Layer Equation, the state of the slow dynamics is assumed to experience little changes in the time scale of the fast dynamics, hence the "slow state" is assumed to be constant in the time scale of the fast system dynamics [27]. The corresponding Layer Equation of (9) is given by

$$C_t\dot{V}_d = -R_L^{-1}V_d + \omega_0 C_t V_q + I_{td} + \mathcal{B}I_d - I_{Ld}b \quad (10a)$$
$$C_t\dot{V}_q = -\omega_0 C_t V_d - R_L^{-1}V_q + I_{tq} + \mathcal{B}I_q - I_{Lq}b \quad (10b)$$
$$L_t\dot{I}_{td} = -V_d - R_t I_{td} + \omega_0 L_t I_{tq} + u_d \quad (10c)$$
$$L_t\dot{I}_{tq} = -V_q - \omega_0 L_t I_{td} - R_t I_{tq} + u_q \quad (10d)$$
$$L\dot{I}_d = -\mathcal{B}^T V_d - RI_d + \omega_0 L I_q \quad (10e)$$
$$L\dot{I}_q = -\mathcal{B}^T V_q - \omega_0 L I_d - RI_q \quad (10f)$$
$$\dot{b} = A(\xi - b - Hs) \quad (10g)$$
$$\dot{\xi}(t) = 0, \text{ for } t \in [t_k, t_{k+1}) \quad (11a)$$
$$\xi(t_k) = m(t_k) \quad (11b)$$
$$\dot{m}(t) = C\Big(v^{\text{hed}} - m(t)\Big) + D\Big(v^{\text{bio}} - m(t)\Big), \quad (11c)$$

where $\xi(t) \in \mathbb{R}^N$, $t_k \in \{t_0, t_1, \ldots\}$ with $k \in \mathbb{Z}_{\geq 0}$ is a time instant such that in the time interval $[t_k, t_{k+1})$, m can be considered constant. In principle, the smaller $t_{k+1} - t_k$, the better the approximation of (10)–(11) to (9). Specifically, (10) and (11) represent fast and slow dynamics, respectively. By (10), one can inspect the dynamics of the microgrid for each $[t_k, t_{k+1})$. As $t_k \to \infty$, the long-term influence of human values on microgrids can be visible, as will also be shown by simulation.

Similarly, one can obtain the corresponding Layer Equation considering case ii) by replacing (11c) with (8b).

In practice, some problems need to be investigated in short and/or long time windows. The problems related to short term performance (with a time scale of milliseconds or seconds) of microgrids have been extensively studied, e.g., in [17], while the problems regarding microgrids in long term have also been investigated, e.g., in the papers [29], [30], in which "long term" refers to a time scale ranging from half to several minutes. In the field of energy planing, some problems are analyzed from the perspective of long and short time windows, where the long time window refers to a decade and short one refers to one year [31], [32]. As an inter disciplinary work, our system model (e.g., (9) and (10)-(11)) fills in the gap between the two cases, i.e., we are able to study the control problem regarding the part of microgrids in a short time window, and study the overall problem regarding the human-in-the-loop system in a longer time window. Although one can study the control of microgrids and human activities separately as in conventional studies, our model provides useful control-oriented insights about the interplay between the physical system and the human in both short and long time horizons, e.g., inspecting the real-time electrical signals influenced by human activities and predicting future energy behaviors. As will be shown in the next two sections, the system (10), (11) is the foundation for the formulation of a social-physical optimization problem and the design of a primal-dual controller to solve it, which constitute the cyber layer of the proposed framework.

III. Optimization Problem

In this section we formulate the optimization problem associated with (10), (11), taking into account both physical and social aspects.

A. Physical Welfare

In this subsection, we introduce the control objective of voltage regulation and a cost function associated with the minimization of current generation.

We consider the regulation of V_d and V_q. Let $V_g^r = [V_{g1}^r, \ldots, V_{gN}^r]^T \in \mathbb{R}^N_{\geq 0}$ be the vector of voltage references for V_g, with $g = d, q$. We assume that V_d^r and V_q^r are provided by an upper control layer. We would like to achieve exact voltage regulation at the steady state, i.e., $\lim_{t\to\infty} V_{di}(t) = V_{di}^r$ and $\lim_{t\to\infty} V_{qi}(t) = V_{qi}^r$ for $i = 1, 2, \ldots, N$.

Furthermore, we assume that the cost function associated with the generation of current is given by

$$C(I_{td}, I_{tq}) := \sum_{i\in\mathcal{N}} \frac{1}{2}\pi_{ci}\Big(I_{tdi}^2 + I_{tqi}^2\Big), \quad (12)$$

where $\pi_{ci} > 0$ represents the unit cost of current generation of prosumer i.

Given any constant V_d^r, V_q^r and $\bar{s}$, and assuming that $\bar{V}_d = V_d^r$ and $\bar{V}_q = V_q^r$ by control, the steady-state of the microgrid (10) in the interval $[t_k, t_{k+1})$ satisfies

$$\bar{u}_d = \bar{V}_d + R_t\bar{I}_{td} - \omega_0 L_t\bar{I}_{tq} \quad (13a)$$
$$\bar{u}_q = \bar{V}_q + \omega_0 L_t\bar{I}_{td} + R_t\bar{I}_{tq} \quad (13b)$$
$$\bar{I}_{td} = I_{Ld}\bar{b} + \Big(R_L^{-1} + \mathcal{B}J_1\mathcal{B}^T\Big)\bar{V}_d + \big(\mathcal{B}J_2\mathcal{B}^T - \omega_0 C_t\big)\bar{V}_q \quad (13c)$$
$$\bar{I}_{tq} = I_{Lq}\bar{b} + \big(\omega_0 C_t - \mathcal{B}J_2\mathcal{B}^T\big)\bar{V}_d + \Big(\mathcal{B}J_2\mathcal{B}^T - R_L^{-1}\Big)\bar{V}_q \quad (13d)$$
$$\bar{b} = \xi - H\bar{s}, \quad (13e)$$

where $J_1 = (R^2 + \omega_0^2 L^2)^{-1}R$ and $J_2 = (R^2 + \omega_0^2 L^2)^{-1}\omega_0 L \in \mathbb{R}^{E\times E}$. Note that $\bar{I}_d = (R^2 + \omega_0^2 L^2)^{-1}(-R\mathcal{B}^T\bar{V}_d - \omega_0 L\mathcal{B}^T\bar{V}_q)$ and $\bar{I}_q = (R^2 + \omega_0^2 L^2)^{-1}(\omega_0 L\mathcal{B}^T\bar{V}_d - R\mathcal{B}^T\bar{V}_q)$ have been substituted in (13). Note also that the steady-state of the microgrid in (13) depends on $\xi(t) = m(t_k) = [m_1(t_k) \ldots m_i(t_k) \ldots m_N(t_k)]^T$ in $[t_k, t_{k+1})$, where $m_i(t_k)$ can be obtained from (11). Overall, from (13) and $\xi(t) = m(t_k)$, one can verify that given $(\xi, \bar{s}, \bar{u}_d, \bar{u}_q)$, the forced equilibrium of the Layer Equation (10)–(11) exists and is unique.

B. Social Welfare

In this subsection, we formulate the social (and economic) welfare problem within the considered microgrid.

First, let $I_{Li} := (I_{Ldi}^2 + I_{Lqi}^2)^{1/2}$. Then, we assign to every prosumer a strictly concave quadratic 'utility' function $U_i(b_i)$ depending on the load satisfaction of prosumer i. Then, the overall utility can be expressed as

$$U(b) := -\sum_{i\in\mathcal{N}} \frac{1}{2}\pi_{ui}(I_{Li}(\xi_i - b_i))^2, \quad (14)$$

where the parameter $\pi_{ui} \in \mathbb{R}_{\geq 0}$ weights the satisfaction of the load demand of prosumer i. For example, a relatively large π_{ui} corresponds to a relatively large request of comfort from prosumer i (see [15] for suggestions on how to select the parameters π_{ui}). By minimizing $-U(b)$, we aim at satisfying prosumers' load demands as much as possible by making $\bar{b}$ close to ξ in $[t_k, t_{k+1})$ (i.e., making $\xi_i - \bar{b}_i$ close to 0).

We would also like to guarantee that the intervention s is close to a given reference value $s_r \in \mathbb{R}^N$. In this paper, we let $s_r = [s_1^r, \ldots, s_N^r]^T$ be a constant vector, which can represent, e.g., the recommended intervention provided by a higher-layer control system or external parties such as the government or energy provider. Accordingly, we aim at minimizing the cost function $\|s - s_r\|^2$. In simulation, we will also show the effectiveness of time-varying s_r.

C. Social-Physical Welfare

Considering the physical and social welfares in Sections III-A and III-B, respectively, we now formulate the overall social-physical welfare optimization problem. Let the optimization variables be denoted by the superscript * and let $\hat{x}_c := [b^{*T}\, I_{td}^{*T}\, I_{tq}^{*T}\, u_d^{*T}\, u_q^{*T}\, s^{*T}]^T \in \mathbb{R}^{6N}$ be the vector of the optimization variables. Then, in view of the equalities in (13), we consider the following convex minimization problem:

$$\min_{\hat{x}_c} \quad \mathcal{F}(\hat{x}_c) \tag{15a}$$

$$\text{s.t.} \quad \mathbf{0} = I_{Ld}\bar{b}^* - \bar{I}_{td}^* + J_3 V_d^r + J_4 V_q^r \tag{15b}$$

$$\mathbf{0} = I_{Lq}\bar{b}^* - \bar{I}_{tq}^* - J_4 V_d^r + J_5 V_q^r \tag{15c}$$

$$\mathbf{0} = V_d^r + R_t\bar{I}_{td}^* - \omega_0 L_t \bar{I}_{tq}^* - \bar{u}_d^* \tag{15d}$$

$$\mathbf{0} = V_q^r + \omega_0 L_t \bar{I}_{td}^* + R_t\bar{I}_{tq}^* - \bar{u}_q^* \tag{15e}$$

$$\mathbf{0} = \xi - \bar{b}^* - H\bar{s}^*, \tag{15f}$$

for $[t_k, t_{k+1})$, where $J_3 = R_L^{-1} + \mathcal{B}J_1\mathcal{B}^T$, $J_4 = -\omega_0 C_t + \mathcal{B}J_2\mathcal{B}^T$, $J_5 = -R_L^{-1} + \mathcal{B}J_2\mathcal{B}^T \in \mathbb{R}^{N\times N}$ and

$$\mathcal{F} := \frac{1}{2}\alpha \sum \pi_{ui} I_{Li}^2 \left(\xi_i - b_i^*\right)^2 + \frac{1}{2}\beta \sum \pi_{ci}\left(I_{tdi}^{*2} + I_{tqi}^{*2}\right) + \frac{\gamma}{2}\|u_d^*\|^2 + \frac{\delta}{2}\|u_q^*\|^2 + \frac{\eta}{2}\|s^* - s_r\|^2. \tag{16}$$

In (16), α, β, γ, δ and η are positive constants that can be chosen to prioritize one objective over another. The terms depending on u_d^* and u_q^* concern the minimization of the control efforts. Note that the supply-demand balance can be adjusted by tuning the parameters α, β, γ, δ and η. For example, if one would like to achieve a supply-demand balance such that the prosumers' demand is satisfied as much as possible, then α needs to be selected relatively "large" with respect to the other parameters. Furthermore, we note that in addition to the equality constraints (15b)–(15f), inequality constraints (see, e.g., [16]) may also be considered for instance to avoid line congestion or too high incentives that are financially unsustainable and undesirable, which will be considered in the future. Note also that, from (13a)–(13b) and (15d)–(15e), it follows that when the optimization problem (15) is solved, then the obtained $\bar{u}_{d,q}^* = \bar{u}_{d,q}$ implies $\bar{V}_d = \bar{V}_d^r$ and $\bar{V}_q = \bar{V}_q^r$.

IV. Controller Design and Stability Analysis

In this section we complete the development of the cyber layer by designing a primal-dual controller that solves the optimization problem (15). Then, we analyze the stability of the overall HCPS framework.

A. Design of a Primal-Dual Controller

Let $\lambda := [\lambda_a^T\, \lambda_b^T\, \lambda_c^T\, \lambda_d^T\, \lambda_e^T]^T \in \mathbb{R}^{5N}$ denote the vector of the Lagrange multipliers corresponding to the constraints in (15b)–(15f). Moreover, let $x_c := [\hat{x}_c^T\, \lambda^T]^T \in \mathbb{R}^{11N}$ be the state vector of the primal-dual controller that we will design later in this subsection. Then, the Lagrangian function corresponding to the optimization problem (15) is the following

$$\begin{aligned}\ell(x_c) :=\ & \mathcal{F}(\hat{x}_c) + \lambda_a^T\left(I_{Ld}\bar{b}^* - \bar{I}_{td}^* + J_3 V_d^r + J_4 V_q^r\right) \\ &+ \lambda_b^T\left(I_{Lq}\bar{b}^* - \bar{I}_{tq}^* - J_4 V_d^r + J_5 V_q^r\right) \\ &+ \lambda_c^T\left(V_d^r + R_t\bar{I}_{td}^* - \omega_0 L_t \bar{I}_{tq}^* - \bar{u}_d^*\right) \\ &+ \lambda_d^T\left(V_q^r + \omega_0 L_t \bar{I}_{td}^* + R_t\bar{I}_{tq}^* - \bar{u}_q^*\right) + \lambda_e^T\left(\xi - b^* - Hs^*\right).\end{aligned} \tag{17}$$

Thus, the first order optimality conditions for the optimization problem (15) are given by the Karush-Kuhn-Tucker (KKT) conditions, i.e.,

$$\mathbf{0} = -\alpha\Pi_u I_L^2\left(\xi - \bar{b}^*\right) + I_{Ld}\bar{\lambda}_a + I_{Lq}\bar{\lambda}_b - \bar{\lambda}_e \tag{18a}$$

$$\mathbf{0} = \beta\Pi_c\bar{I}_{td}^* - \bar{\lambda}_a + R_t\bar{\lambda}_c + \omega_0 L_t\bar{\lambda}_d \tag{18b}$$

$$\mathbf{0} = \beta\Pi_c\bar{I}_{tq}^* - \bar{\lambda}_b - \omega_0 L_t\bar{\lambda}_c + R_t\bar{\lambda}_d \tag{18c}$$

$$\mathbf{0} = \gamma\bar{u}_d^* - \bar{\lambda}_c \tag{18d}$$

$$\mathbf{0} = \delta\bar{u}_q^* - \bar{\lambda}_d \tag{18e}$$

$$\mathbf{0} = \eta\left(\bar{s}^* - s_r\right) - \bar{\lambda}_e \tag{18f}$$

$$\mathbf{0} = I_{Ld}\bar{b}^* - \bar{I}_{td}^* + J_3\bar{V}_d^r + J_4 V_q^r \tag{18g}$$

$$\mathbf{0} = I_{Lq}\bar{b}^* - \bar{I}_{tq}^* - J_4\bar{V}_d^r + J_5 V_q^r \tag{18h}$$

$$\mathbf{0} = V_d^r + R_t\bar{I}_{td}^* - \omega_0 L_t\bar{I}_{tq}^* - \bar{u}_d^* \tag{18i}$$

$$\mathbf{0} = V_q^r + \omega_0 L_t\bar{I}_{td}^* + R_t\bar{I}_{tq}^* - \bar{u}_q^* \tag{18j}$$

$$\mathbf{0} = \xi - \bar{b}^* - H\bar{s}^*, \tag{18k}$$

with $\Pi_u = \text{diag}(\pi_{u1}, \ldots, \pi_{uN})$, $\Pi_c = \text{diag}(\pi_{c1}, \ldots, \pi_{cN})$ and $I_L^2 = \text{diag}(I_{L1}^2, \ldots, I_{LN}^2)$. Since the optimization problem (15) is convex, then strong duality holds [33]. Thus, $\bar{b}^*, \bar{I}_{td}^*, \bar{I}_{tq}^*, \bar{u}_d^*, \bar{u}_q^*, \bar{s}^*$ are optimal if and only if there exist $\bar{\lambda}_a, \bar{\lambda}_b, \bar{\lambda}_c, \bar{\lambda}_d$ and $\bar{\lambda}_e$ that satisfy (18).

Based on the KKT conditions in (18) and under the assumption that each controller can exchange information among its neighbors through a communication network with the same topology as the physical network, we design the following *distributed control scheme* by using the primal-dual dynamics of the optimization problem (15), i.e.,

$$-\tau_b\dot{b}^* = -\alpha\Pi_u I_L^2\left(\xi - b^*\right) + I_{Ld}\lambda_a + I_{Lq}\lambda_b - \lambda_e \tag{19a}$$

$$-\tau_{td}\dot{I}_{td}^* = \beta\Pi_c I_{td}^* - \lambda_a + R_t\lambda_c + \omega_0 L_t\lambda_d \tag{19b}$$

$$-\tau_{tq}\dot{I}_{tq}^* = \beta\Pi_c I_{tq}^* - \lambda_b - \omega_0 L_t\lambda_c + R_t\lambda_d \tag{19c}$$

$$-\tau_{ud}\dot{u}_d^* = \gamma u_d^* - \lambda_c + \phi_A \tag{19d}$$

$$-\tau_{uq}\dot{u}_q^* = \delta u_q^* - \lambda_d + \phi_B \tag{19e}$$

$$-\tau_s\dot{s}^* = \eta\left(s^* - s_r\right) - \lambda_e + \phi_C \tag{19f}$$

$$\tau_a\dot{\lambda}_a = I_{Ld}b^* - I_{td}^* + J_3V_d^r + J_4V_q^r \tag{19g}$$
$$\tau_b\dot{\lambda}_b = I_{Lq}b^* - I_{tq}^* - J_4V_d^r + J_5V_q^r \tag{19h}$$
$$\tau_c\dot{\lambda}_c = V_d^r + R_tI_{td}^* - \omega_0L_tI_{tq}^* - u_d^* \tag{19i}$$
$$\tau_d\dot{\lambda}_d = V_q^r + \omega_0L_tI_{td}^* + R_tI_{tq}^* - u_q^* \tag{19j}$$
$$\tau_e\dot{\lambda}_e = \xi - b^* - Hs^*, \tag{19k}$$

where $\tau_b, \tau_{td}, \tau_{tq}, \tau_{ud}, \tau_{uq}, \tau_s, \tau_a, \tau_b, \tau_c, \tau_d, \tau_e \in \mathbb{R}^{N\times N}$ are positive diagonal matrices, which can be tuned to adjust the controller response. Moreover, the vectors ϕ_A, ϕ_B and ϕ_C are the controller input ports, which will be used in the next subsection to interconnect the controller (19) with (10) and (11). We also note that since in the optimization problem (15) the objective function (16) is quadratic with respect to $b^*, I_{td}^*, I_{tq}^*, u_d^*, u_q^*, s^*$ and the constraints (15b)–(15f) are linear, then, given constant $\bar{\phi}_A, \bar{\phi}_B$ and $\bar{\phi}_C$, it can be shown that the solution $\bar{x}_c$ to (19) is unique.

B. Stability Analysis

In this subsection, we will show that (10) and (11) in closed loop with the primal-dual controller (19) are stable and converge to the solution of the optimization problem (15).

The dynamics in (10g) can be written as

$$\dot{b} = -Ab + A(\xi - Hs), \tag{20}$$

with $-A$ being Hurwitz. Thus, given any diagonal and positive definite matrices Q_1, let P_1 denote the corresponding unique solutions of the Lyapunov equation $-A^TP_1 - P_1A + Q_1 = \mathbf{0}$, where P_1 is a positive definite matrix. Then, we interconnect the controller (19) with (10), (11) by choosing

$$u_d = u_d^*,\ u_q = u_q^*,\ s = s^* \tag{21}$$
$$\phi_A = I_{td},\ \phi_B = I_{tq},\ \phi_C = -2H^TA^TP_1^Tb. \tag{22}$$

Note that the controller (19), the interconnections (21)-(22) and the communication network for exchanging data form the cyber layer. By (22), one can see that to control the HCPS as shown in Figure 1, the controller (19) needs to collect I_{td} and I_{tq} from the physical layer (1), (2) and collect b from the human layer (5). Meanwhile, the controller generates control inputs u_d and u_q for the physical layer and s for the human layer. Then, it is clear that the cyber layer interconnects the physical and human layers as shown in Figure 1. Let $x_s := [V_d^T\ V_q^T\ I_{td}^T\ I_{tq}^T\ I_d^T\ I_q^T\ b^T]^T \in \mathbb{R}^{5N+2E}$ denote the state in (10).

Now we are ready to present the main result of this paper.

Theorem 1: The closed-loop system (10), (11), (19), (21) and (22) converges to an equilibrium solving (15).

Proof: We take three steps to conduct the proof.

Step 1: In this step, we first propose the following storage function [34] for the physical system corresponding to (10a)–(10f) as

$$S_p = \frac{1}{2}\Big(\dot{V}_d^TC_t\dot{V}_d + \dot{V}_q^TC_t\dot{V}_q + \dot{I}_{td}^TL_t\dot{I}_{td} + \dot{I}_{tq}^TL_t\dot{I}_{tq} + \dot{I}_d^TL_t\dot{I}_d + \dot{I}_q^TL_t\dot{I}_q\Big), \tag{23}$$

which satisfies

$$\dot{S}_p = -\dot{V}_d^TR_L^{-1}\dot{V}_d - \dot{V}_q^TR_L^{-1}\dot{V}_q - \dot{I}_{td}^TR_t\dot{I}_{td} - \dot{I}_{tq}^TR_t\dot{I}_{tq} - \dot{I}_d^TR\dot{I}_d - \dot{I}_q^TR\dot{I}_q - \dot{V}_d^TI_{Ld}\dot{b} - \dot{V}_q^TI_{Lq}\dot{b} + \dot{I}_{td}^T\dot{u}_d^* + \dot{I}_{tq}^T\dot{u}_q^* \tag{24}$$

along the solutions to (10a)–(10f). Now, supposing without loss of generality that the loads absorb positive reactive power (i.e., the loads are predominantly inductive rather than capacitive), I_{Lq} is negative definite. Then, by virtue of the Young's inequality [35], we have $-\dot{V}_d^TI_{Ld}\dot{b} - \dot{V}_q^TI_{Lq}\dot{b} \le \dot{V}_d^T\frac{I_{Ld}}{2\zeta_2}\dot{V}_d + \dot{b}^T\frac{\zeta_2I_{Ld}}{2}\dot{b} - \dot{V}_q^T\frac{I_{Lq}}{2\zeta_3}V_q^T - \dot{b}^T\frac{\zeta_3I_{Lq}}{2}\dot{b}$, with ζ_2 and ζ_3 being arbitrary positive reals.

Then, for the dynamics in (20) with ξ in (11), we propose the following storage function $S_h = \dot{b}^TP_1\dot{b}$, which satisfies $\dot{S}_h = -\dot{b}^TQ_1\dot{b} - 2\dot{b}^TP_1AH\dot{s}^*$, along the solutions to (20).

Then, for the overall system (10), the storage function $S_{ph} := S_p + S_h$ satisfies

$$\dot{S}_{ph} \le -\dot{V}_d^T\left(R_L^{-1} - \frac{1}{2\zeta_2}I_{Ld}\right)\dot{V}_d - \dot{V}_q^T\left(R_L^{-1} + \frac{1}{2\zeta_3}I_{Lq}\right)V_q - \dot{b}^T\left(Q_1 - \frac{\zeta_2}{2}I_{Ld} + \frac{\zeta_3}{2}I_{Lq}\right)\dot{b} + \dot{I}_{td}^T\dot{u}_d^* + \dot{I}_{tq}^T\dot{u}_q^* - 2\dot{b}^TP_1AH\dot{s}^* \tag{25}$$

along the solution to (10). Recalling that I_{Ld} and I_{Lq} are bounded, we observe that the terms in the first and second lines can be made nonpositive by selecting sufficiently large ζ_2 and ζ_3, respectively. With the selected ζ_2 and ζ_3, also the terms in the third line can be made nonpositive by selecting a sufficiently large Q_1. Then, we have $\dot{S}_{ph} \le \dot{I}_{td}^T\dot{u}_d^* + \dot{I}_{tq}^T\dot{u}_q^* - 2\dot{b}^TP_1AH\dot{s}^*$, which implies that the system (10) is passive with respect to the supply rate $[\dot{I}_{td}^T\ \dot{I}_{tq}^T\ -2\dot{b}^TP_1AH]\,[\dot{u}_d^{*T}\ \dot{u}_q^{*T}\ \dot{s}^{*T}]^T$ and storage function S_{ph}.

Step 2: In this step, we propose for the primal-dual controller (19) the following storage function

$$S_c = \frac{1}{2}\Big(\dot{b}^{*T}\tau_b\dot{b}^* + \dot{I}_{td}^{*T}\tau_{I_{td}}\dot{I}_{td}^* + \dot{I}_{tq}^{*T}\tau_{I_{tq}}\dot{I}_{tq}^* + \dot{u}_d^{*T}\tau_{u_d}\dot{u}_d^* + \dot{u}_q^{*T}\tau_{u_q}\dot{u}_q^* + \dot{s}^{*T}\tau_s\dot{s}^* + \dot{\lambda}_a^T\tau_a\dot{\lambda}_a + \dot{\lambda}_b^T\tau_b\dot{\lambda}_b + \dot{\lambda}_c^T\tau_c\dot{\lambda}_c + \dot{\lambda}_d^T\tau_d\dot{\lambda}_d + \dot{\lambda}_e^T\tau_e\dot{\lambda}_e\Big), \tag{26}$$

which satisfies $\dot{S}_c \le -\dot{u}_d^{*T}\dot{\phi}_A - \dot{u}_q^{*T}\dot{\phi}_B - \dot{s}^{*T}\dot{\phi}_C$ along the solutions to (19). This implies that the controller (19) is passive with respect to the supply rate $-[\dot{p}_A^T\ \dot{p}_B^T\ \dot{\phi}_C^T][\dot{u}_d^{*T}\ \dot{u}_q^{*T}\ \dot{s}^{*T}]^T$ and storage function S_c, with ϕ_A, ϕ_B and ϕ_C in (22).

Step 3: As the last step, for the closed-loop system (10), (11) and (19) with (21) and (22), we propose $S := S_{ph} + S_c$ as storage function, which satisfies $\dot{S} \le 0$ along the solutions to (10), (11) and (19) with (21) and (22), implying that such solutions are bounded. Therefore, there exists a forward invariant set Ω and by LaSalle's invariance principle the solutions that start in Ω converge to the largest invariant set contained in $\Omega \cap \{(x_s, x_c) \in \mathbb{R}^{16N+2E} |\ \dot{x}_s = \mathbf{0}, \dot{b}^* = \mathbf{0}, \dot{I}_{td}^* = \mathbf{0}, \dot{I}_{tq}^* = \mathbf{0}\ \dot{u}_d^* = \mathbf{0}, \dot{u}_q^* = \mathbf{0}, \dot{s}^* = \mathbf{0}\}$. Then, from (19d), (19e), (19f), (19c) and (19b), it follows that on the largest invariant set $\dot{\lambda}_c, \dot{\lambda}_d, \dot{\lambda}_e, \dot{\lambda}_b$ and $\dot{\lambda}_a$ are also equal to zero, respectively. Finally, observing from (13) and $\xi(t) = m(t_k)$ that $\bar{x}_s$ is uniquely determined by $\bar{u}_d = \bar{u}_d^*, \bar{u}_q = \bar{u}_q^*, \xi = m(t_k)$ in $[t_k, t_{k+1}]$ and $\bar{s} = \bar{s}^*$, we can conclude from (19h)–(19i) that at the steady-state the physical state variables coincide with the corresponding optimization variables.

By (6), one can also obtain that $m_i(t_k) \to \bar{m}_i$ as $t_k \to \infty$, which implies that $\xi \to \bar{m}$ as $t_k \to \infty$. In other words, the primal dual controller solves the optimization problem (15) with $\bar{\xi} = \bar{m}$ in (15f) as $t_k \to \infty$.

Remark 2: The controller in (19) with ϕ_A, ϕ_B and ϕ_C in (22) can be implemented in a distributed way. A local controller needs to exchange only the information of its voltage references V_{di}^r and V_{qi}^r with its neighbors' controllers. This is implied by the terms $J_3 V_d^r$, $J_4 V_q^r$, $J_4 V_d^r$ and $J_5 V_q^r$ in (19g) and (19h).

Remark 3: The proposed framework can also incorporate the scenario in which human motivation may be influenced by contextual factors (see Section II-B) on a short time scale, i.e., the parameters c_i and d_i in (3b) can change depending on the underlying circumstances where people are involved. For instance, in compact form, the matrices C and D in (5b) can change along time as long as they belong to the positive-diagonal-matrix sets $\mathcal{C} \coloneqq \{C_1, C_2, \ldots, C_\sigma\}$ and $\mathcal{D} \coloneqq \{D_1, D_2, \ldots, D_\kappa\}$, respectively, where $\sigma, \kappa \in \mathbb{Z}_{\geq 1}$ are finite integers. Thus, the dynamics regarding m are represented by a switched linear system. The influence of contextual factors can be explained by the following illustrative but suitable example: people might be motivated to increase comfort associated with hedonic values when they arrive at home after a stressful day of work even though getting more comfort may increase the energy consumption. The reasoning behind this behavior is that reducing comfort after a stressful day of work can be perceived as more "costly" than usual, due to the specific context of feeling tired after the stressful work day.

C. HCPS Considering Social Norm

In this subsection, we briefly extend the results of Theorem 1 to case ii), which includes the influence of social norms on the dynamics of people's motivations (see (8b)). Thus, the resulting model consists of (10), (11) in which (11c) is replaced by (8b). With ξ obtained by (11) and the fact that $-(C+D+\mathcal{L})$ is negative definite, the controller in (19) is still applicable to the proposed HCPS including social norms.

Then, the rest of the analysis can be conducted analogously to the proof of Theorem 1. Therefore, the following corollary holds.

Corollary 1: The closed-loop system (10), (11), (19), (21) and (22), where (11c) is replaced by (8b), converges to an equilibrium solving (15).

V. Simulations

We consider an islanded AC microgrid consisting of ten prosumers with parameters in Table III. The values of the parameters of the human layer will be provided in the text below and we aim as future research to identify these values in a similar way to the one proposed in [15]. In the following, we consider three simulation scenarios. Specifically, in Scenario i), we consider the case consisting of the model of the AC microgrid (1) and the model of human behavior and motivation (3). To show the effectiveness of social influence in energy saving, Scenario ii) additionally considers social norms. That is, the corresponding HCPS consists of the model

TABLE III
Coefficients of Prosumers and Lines

	Pros. 1	Pros. 2	Pros. 3	Pros. 4	Pros. 5
C_t (μF)	62.86	62.86	62.86	62.86	62.86
L_t (mH)	2.1	2.0	1.9	1.8	2.1
R_t (mΩ)	40.2	38.7	34.6	31.8	40.1
R_L (Ω)	11	13	11	13	11
I_{Ld} (A)	25	23	35	31	25
I_{Lq} (A)	-12	-15	-10	-18	-12
V_d^r (V)	120 $\sqrt{2}$	120 $\sqrt{2}$	120 $\sqrt{2}$	120 $\sqrt{2}$	120 $\sqrt{2}$
V_q^r (V)	0	0	0	0	0
$\pi_{ci} = \pi_{ui}$	1	1	1	1	1
	Line 1	Line 2	Line 3	Line 4	Line 5
R_k (Ω)	0.25	0.27	0.24	0.26	0.25
L_k (μH)	1.2	1.3	1.8	2.1	1.2

	Pros. 6	Pros. 7	Pros. 8	Pros. 9	Pros. 10
C_t (μF)	62.86	62.86	62.86	62.86	62.86
L_t (mH)	2.02	1.9	1.82	2.1	2.02
R_t (mΩ)	38.7	34.6	31.8	40.2	38.7
R_L (Ω)	13	10.86	13	10.86	13
I_{Ld} (A)	23	35	31	25	23
I_{Lq} (A)	-15	-10	-18	-12	-15
V_d^r (V)	120 $\sqrt{2}$	120 $\sqrt{2}$	120 $\sqrt{2}$	120 $\sqrt{2}$	120 $\sqrt{2}$
V_q^r (V)	0	0	0	0	0
$\pi_{ci} = \pi_{ui}$	1	1	1	1	1
	Line 6	Line 7	Line 8	Line 9	Line 10
R_k (Ω)	0.27	0.24	0.26	0.25	0.27
L_k (μH)	1.3	1.8	2.1	1.2	1.3

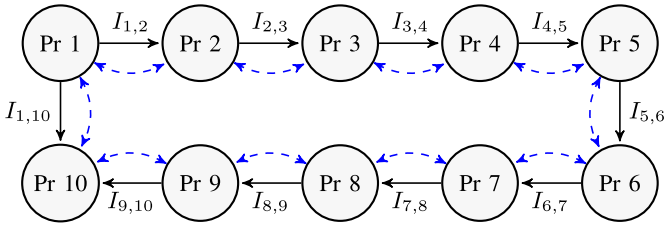

Fig. 3. Scheme of the considered microgrid with 10 prosumers (Pr). The solid arrows indicate the positive direction of the current flows through the power network, while the dashed lines represent the communication network.

of the AC microgrid (1) and the models of human behavior (3a) and motivation (7), and the controller (19) with the ports in (21) and (22). The first two scenarios are meaningful because, given constant nominal loads, we can still observe a dynamical behavior due to human activities. Different from Scenarios i) and ii), where the nominal load is time-invariant, in Scenario iii), we consider a more realistic situation in practice, where the nominal load is time-varying (i.e., I_L is considered as a time-dependent external input) and load data are taken from the database of power consumption of New York Central Park [36]. Moreover, differently from Scenarios i) and ii), in Scenario iii) we make the intervention reference s_r time-varying as well, in order to encourage prosumers to decrease the power consumption during the peak hours, and increase the power consumption during the off-peak hours. The influence of contextual factors on energy consumption is also considered.

Scenario i) The parameters for the human motivation-behavior model are selected as follows, $A = 110 \times \mathbf{I}^{10\times 10}$ indicating the time constant of the behavior dynamics,

$$C = 10^{-4} \times \text{diag}(0.14\ 0.14\ 0.16\ 0.16\ 0.144\ 0.144\ 0.16\ 0.16\ 0.148\ 0.148)$$

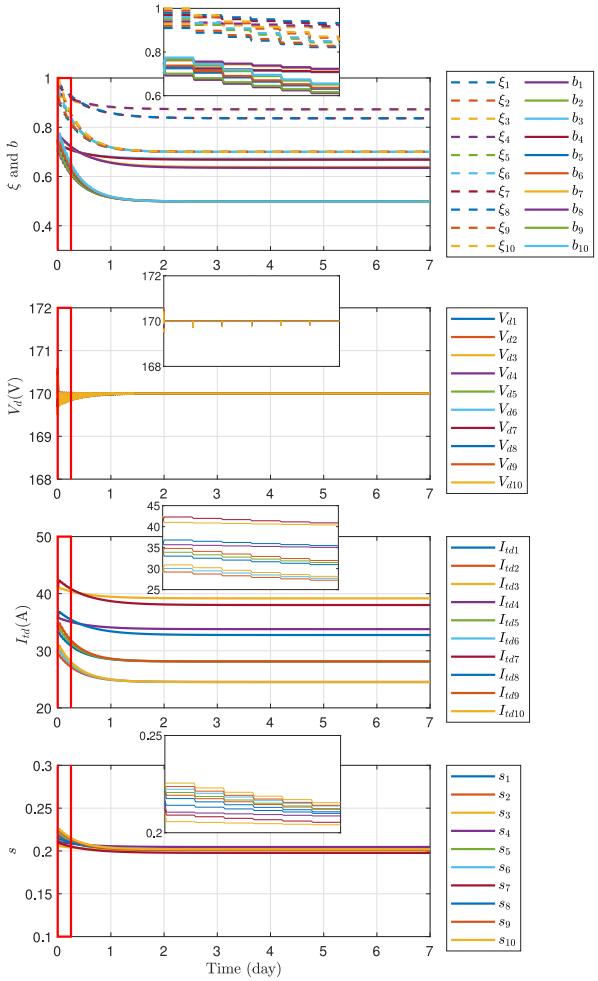

Fig. 4. Scenario i). The system dynamics in the first 6 hours (in red rectangular) are zoomed-in and shown in the small windows for showing the dynamics changing by hours.

$$D = 10^{-4} \times \text{diag}(0.16\ 0.16\ 0.06\ 0.06\ 0.162\ 0.162\ 0.06\ 0.06\ 0.164\ 0.164)$$

specifying the weights of hedonic and biospheric values, respectively. Moreover, we select

$$v^{\text{hed}} = [0.7\ 0.7\ 0.81\ 0.81\ 0.72\ 0.72\ 0.8\ 0.8\ 0.74\ 0.74]^T$$
$$v^{\text{bio}} = [0.7\ 0.7\ 0.8\ 0.8\ 0.7\ 0.7\ 0.8\ 0.8\ 0.7\ 0.7]^T,$$

indicating the prosumers' hedonic values and biospheric values, respectively. Let $t_{k+1} - t_k = 1\text{h}$ indicating the time interval of the Layer Equation (10)–(11) approximating (9).

The simulation results for Scenario i) are presented in Figure 4. In each plot of Figure 4, we also show an enlargement of the first 6 hours in order to make the transient dynamics clearly visible. In the enlargements, we observe that the dynamics of the states are piece-wise constant, which is the consequence of the selection of $t_{k+1} - t_k = 1\text{h}$ in the Layer Equation (10)–(11). Note that one can choose different time intervals for $t_{k+1} - t_k$ depending on the specific approximation of the demand. In the first plot of Figure 4, we observe that due to the influence of biospheric values v^{bio}, the motivation ξ of prosumers indeed decreases and finally reaches a steady-state

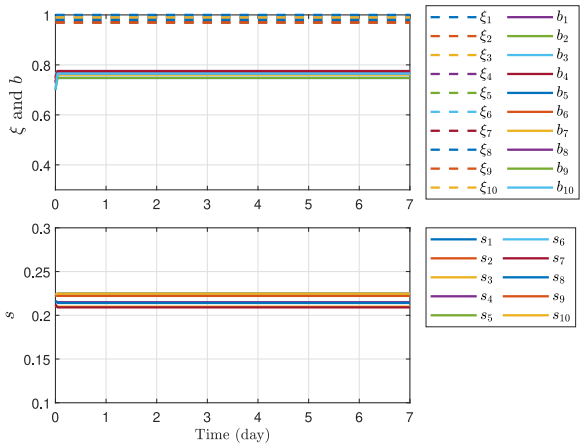

Fig. 5. Constant motivation.

value. Due to intervention s_i (approximately equal to ~ 0.2) shown in the forth plot of Figure 4, the power consumption is lower than the amount that they would have consumed in the absence of the interventions. This can be observed from the first plot of Figure 4, where the values of behaviors b_i are smaller than the corresponding motivations ξ_i, and the reduced value corresponds to s_i. Moreover, the obtained s_i is very close to the given reference value of intervention $s_r = 0.2 \times \mathbf{1}_{10}^T$ (see the fourth plot in Figure 4).

Now we discuss the performance of the AC microgrid. We show the voltage trajectories in the second plot of Figure 4, where the voltage V_d is stabilized around the reference value $V_d^r = 120\sqrt{2}$ V. Moreover, due to the "decreasing" motivation-behavior dynamics shown in the first plot of Figure 4, the absorbed current $I_{Ldi}b_i$ is time-varying and decreases, and consequently the current generation is also time-varying and decreases as well (see the third plot in Figure 4). Finally, note that we have verified in simulation that $V_q \to \mathbf{0}$, but omit the corresponding plot due to page limit.

For the sake of comparison, we present in Figure 5 the simulation results obtained by considering the motivation m to be constant $\mathbf{1}_N^T$ with random variations. This is done to simulate the scenario where the influence of human personal values are not taken into account and the reduction of power consumption is purely driven by intervention. First, note that the values of intervention s in Figure 5 are larger than those in the fourth plot of Figure 4 under the same reference s_r, which means a larger cost for intervention. More importantly, with a larger cost for intervention, the values of b are still larger than those in the first plot of Figure 4, which implies more power consumption. Indeed, the prosumers in this case consume 2139 kWh more. This reveals that, if one omits the influence of human values, it is highly possible that the government/society estimation of cost for intervention will be higher, and the energy consumption will not be necessarily lower. If we consider b to be constant as well, where the value of b is directly determined by solving the optimization problem, instead of dynamically depending on s, then, one recovers the problem in [15].

Scenario ii) In this scenario, we additionally consider the influence of social norms. For the social network topology among the prosumers, we select $\mathcal{L} = 0.6 \cdot 10^{-4} \times \mathcal{B}\mathcal{B}^T$ in (8b).

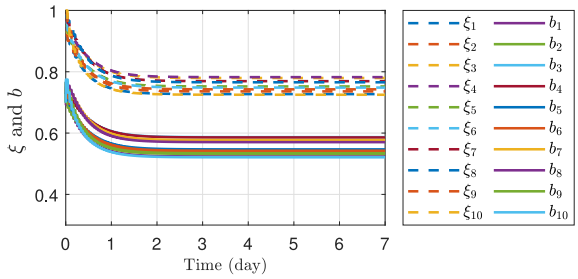

Fig. 6. Scenario ii) with considering the influence of social norms.

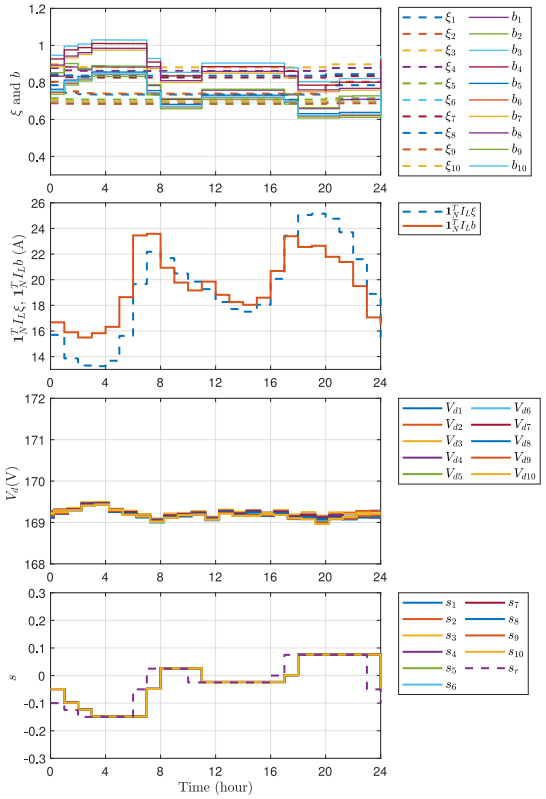

Fig. 7. Case iii). Time-varying load and intervention reference.

The other parameters are as in Scenario i). We show the time evolution of the motivation ξ (in Layer Equation) and behavior b in Figure 6 and omit the other signals due to the similarity to those in Scenario i). Since the Laplacian matrix $\mathcal{L}$ in (8b) represents a connected and undirected graph, one can see that the components in ξ and b in Figure 6 converge to values that are closer to each other with respect to those in the first plot of Figure 4 in Scenario i). Similarly to Scenario i), in Figure 6 one can observe that the discrepancy between ξ_i and b_i is approximately 0.2, which is the consequence of the intervention s_i. Due to the influence of social norms, it is possible to calculate that the energy consumption of each prosumer in the considered time horizon of 7 days is reduced by 2.55 kWh/day in average than that in Scenario i).

Scenario iii) Compared with Scenarios i) and ii), where the nominal loads and behavior interventions are time-invariant, this scenario is more realistic and considers time-varying nominal loads, time-varying behavior interventions, and also the influence of contextual factors. Specifically, we simulate the

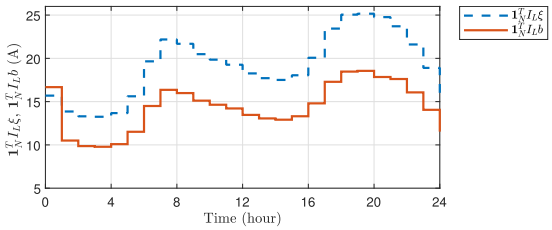

Fig. 8. Static reference values of intervention.

case of time-varying nominal loads (i.e., time-varying I_L), where load data are taken from the database of power consumption of the area of New York Central Park [36]. The simulation results are shown in Figure 7. Furthermore, we consider the influence of contextual factors in order to take into account the effects of human motivation also on a shorter time scale, due for example to the fact that during some hours of the day one can more or less strongly endorse a value rather than another. It is indeed reasonable to expect that due to adversary weather conditions and/or a stressful working day, the influence of the hedonic values on human motivation may be stronger. For this, we choose

$$C = \text{diag}(1.66\ 1.68\ 3.1\ 3.2\ 1.68\ 1.7\ 3.3\ 3.3\ 1.7\ 1.67) \times 10^{-4}$$
$$D = \text{diag}(2.92\ 2.92\ 1.25\ 1.25\ 2.92\ 2.92\ 1.25\ 1.25\ 2.92\ 2.92) \times 10^{-4}$$

from 24 to 19 o'clock, and

$$C = \text{diag}(6.8\ 6.9\ 9\ 9\ 6.6\ 6.7\ 10\ 10\ 6.9\ 6.6\ ) \times 10^{-4}$$
$$D = \text{diag}(2.91\ 2.92\ 1.25\ 1.24\ 2.8\ 2.95\ 1.25\ 1.25\ 2.9\ 2.92) \times 10^{-4}$$

from 19 to 24 o'clock, which corresponds to the scenario in which the prosumers increase the energy consumption in order to acquire pleasure and comfort, for instance when they arrive at home after a stressful work day. This is shown in the first plot of Figure 7, in which the motivation ξ (dashed lines) from 19 to 24 o'clock is slightly larger than those of other times. Different from Scenarios i) and ii), where we considered a constant intervention reference s_r, in this scenario we consider the intervention reference s_r to be time-varying during the day, as shown in the fourth plot of Figure 7. Specifically, one can see that in the example we introduce "negative" reference for encouraging the use of energy during the midnight and "positive" reference for encouraging energy saving during the evening. The benefits of time-varying intervention reference s_r and the corresponding effect on s can be observed from the second plot in Figure 7, where prosumers shift the time of consuming energy by using more energy during the midnight and less during the day compared to the case of static intervention. Specifically, the actual current load $\mathbf{1}_N^T I_L b$ (solid lines) is smaller than the current load $\mathbf{1}_N^T I_L \xi$ that people would have consumed (dashed lines) during the peak hours in the evening, and larger than the current load $I_L \xi$ that people would have consumed in the midnight. Thus one can see that, by a suitable choice of s_r, it is possible to shift the use of energy from the peak hours to the off-peak ones. If one applies a static s_r, it is difficult to shift the use of energy and one still has peak hours (i.e., the evening),

though the peak is reduced by the static s_r (see the orange line in Figure 8). Finally, from the third plot in Figure 7, we can observe that the voltage V_d is stabilized around the reference voltage value $V_d^r = 120\sqrt{2}$V. Note that the controller (19) becomes a time-varying system in Scenario iii) instead of a time-invariant system leading to Theorem 1.

VI. Conclusion

We have developed a framework to bridge the disciplines of systems & control and psychology to jointly study energy dynamical behavior of human together with the dynamics of the microgrid. Specifically, we have formulated a HCPS framework to describe energy behavior of humans in social networks and also their interactions with the microgrid via a cyber layer. The developed models describing human energy behavior depend on motivation and behavioral interventions, and are consistent with the findings in psychology. With the developed HCPS, we have formulated a social-physical welfare optimization problem and have designed a distributed primal-dual control scheme. It is proven that the proposed control system generates the optimal intervention to humans and control inputs to the microgrid, stabilizing the closed-loop system whose state converges to an equilibrium solving the considered optimization problem. The HCPS framework shows that human intrinsic factors (values and motivation) and behaviours can have substantial impact on the energy system and should therefore be accounted for in energy system modelling. The results in this paper have also shown the interplay among human, physical systems, energy consumption and a player providing references for interventions. The developed models of human activities not only interpret the findings in psychology from the control viewpoint, but also are consistent with the studies on opinion dynamics.

Interesting future research includes the design and analysis of HCPS frameworks to embed the proposed human layer into analogous optimization control problems for the main grid (e.g., [16]) or DC microgrids (e.g., [37]). Additionally, different operation modes and control objectives can be considered, e.g., the grid-connected operation mode and power sharing objective. One can also expand the current human motivation-behavior models by including variables/factors from prominent psychological models, such as the value belief norm theory [24] and norm activation model [38].

References

[1] L. Steg, G. Perlaviciute, and E. van der Werff, "Understanding the human dimensions of a sustainable energy transition," *Front. Psychol.*, vol. 6, p. 805, Jun. 2015.

[2] P. C. Stern, K. B. Janda, M. A. Brown, L. Steg, E. L. Vine, and L. Lutzenhiser, "Opportunities and insights for reducing fossil fuel consumption by households and organizations," *Nat. Energy*, vol. 1, no. 5, pp. 1–6, 2016.

[3] N. Ahmed, M. Levorato, and G.-P. Li, "Residential consumer-centric demand side management," *IEEE Trans. Smart Grid*, vol. 9, no. 5, pp. 4513–4524, Sep. 2018.

[4] E. Thomas, R. Sharma, and Y. Nazarathy, "Towards demand side management control using household specific Markovian models," *Automatica*, vol. 101, pp. 450–457, Mar. 2019.

[5] M. Ghorbaniparvar, X. Li, and N. Zhou, "Demand side management with a human behavior model for energy cost optimization in smart grids," in *Proc. IEEE Global Conf. Signal Inf. Process. (GlobalSIP)*, 2015, pp. 503–507.

[6] B. Hayes, I. Melatti, T. Mancini, M. Prodanovic, and E. Tronci, "Residential demand management using individualized demand aware price policies," *IEEE Trans. Smart Grid*, vol. 8, no. 3, pp. 1284–1294, May 2017.

[7] P. Sheeran, "Intention–behavior relations: A conceptual and empirical review," *Eur. Rev. Soc. Psychol.*, vol. 12, no. 1, pp. 1–36, 2002.

[8] T. Dietz, A. Fitzgerald, and R. Shwom, "Environmental values," *Annu. Rev. Environ. Resour.*, vol. 30, pp. 335–372, Nov. 2005.

[9] D. Schwartz, W. B. de Bruin, B. Fischhoff, and L. Lave, "Advertising energy saving programs: The potential environmental cost of emphasizing monetary savings," *J. Exp. Psychol. Appl.*, vol. 21, no. 2, pp. 158–166, 2015.

[10] J. M. Nolan, P. W. Schultz, R. B. Cialdini, N. J. Goldstein, and V. Griskevicius, "Normative social influence is underdetected," *Pers. Soc. Psychol. Bull.*, vol. 34, no. 7, pp. 913–923, 2008.

[11] P. W. Schultz, J. M. Nolan, R. B. Cialdini, N. J. Goldstein, and V. Griskevicius, "The constructive, destructive, and reconstructive power of social norms," *Psychol. Sci.*, vol. 18, no. 5, pp. 429–434, 2007.

[12] L. Steg and C. Vlek, "Encouraging pro-environmental behaviour: An integrative review and research agenda," *J. Environ. Psychol.*, vol. 29, no. 3, pp. 309–317, 2009.

[13] N. E. Friedkin and E. C. Johnsen, "Social influence and opinions," *J. Math. Sociol.*, vol. 15, nos. 3–4, pp. 193–206, 1990.

[14] M. Ye, M. H. Trinh, Y.-H. Lim, B. D. O. Anderson, and H.-S. Ahn, "Continuous-time opinion dynamics on multiple interdependent topics," *Automatica*, vol. 115, May 2020, Art. no. 108884.

[15] M. Cucuzzella et al., "Distributed control of DC grids: Integrating prosumers' motives," *IEEE Trans. Power Syst.*, vol. 37, no. 4, pp. 3299–3310, Jul. 2022.

[16] T. Stegink, C. De Persis, and A. J. van der Schaft, "A unifying energy-based approach to stability of power grids with market dynamics," *IEEE Trans. Autom. Control*, vol. 62, no. 6, pp. 2612–2622, Jun. 2017.

[17] C. Zhao, U. Topcu, N. Li, and S. Low, "Design and stability of load-side primary frequency control in power systems," *IEEE Trans. Autom. Control*, vol. 59, no. 5, pp. 1177–1189, May 2014.

[18] R. H. Park, "Two-reaction theory of synchronous machines generalized method of analysis—part I," *Trans. Amer. Inst. Electr. Eng.*, vol. 48, no. 3, pp. 716–727, Jul. 1929.

[19] M. Cucuzzella, S. Trip, A. Ferrara, and J. Scherpen, "Cooperative voltage control in AC microgrids," in *Proc. IEEE Conf. Decis. Control*, 2018, pp. 6723–6728.

[20] D.-M. Han and J.-H. Lim, "Design and implementation of smart home energy management systems based on ZigBee," *IEEE Trans. Consum. Electron.*, vol. 56, no. 3, pp. 1417–1425, Aug. 2010.

[21] S. H. Schwartz et al., "Refining the theory of basic individual values," *J. Pers. Soc. Psychol.*, vol. 103, no. 4, pp. 663–688, 2012.

[22] P. C. Stern and T. Dietz, "The value basis of environmental concern," *J. Soc. Issues*, vol. 50, no. 3, pp. 65–84, 1994.

[23] E. Dogan, J. W. Bolderdijk, and L. Steg, "Making small numbers count: Environmental and financial feedback in promoting eco-driving behaviours," *J. Consum. Policy*, vol. 37, no. 3, pp. 413–422, 2014.

[24] P. C. Stern, "New environmental theories: Toward a coherent theory of environmentally significant behavior," *J. Soc. Issues*, vol. 56, no. 3, pp. 407–424, 2000.

[25] L. Steg, J. W. Bolderdijk, K. Keizer, and G. Perlaviciute, "An integrated framework for encouraging pro-environmental behaviour: The role of values, situational factors and goals," *J. Environ. Psychol.*, vol. 38, pp. 104–115, Jun. 2014.

[26] C. Cenedese, F. Fabiani, M. Cucuzzella, J. M. A. Scherpen, M. Cao, and S. Grammatico, "Charging plug-in electric vehicles as a mixed-integer aggregative game," in *Proc. IEEE 58th Conf. Decis. Control (CDC)*, 2019, pp. 4904–4909.

[27] H. Jardón-Kojakhmetov, J. M. A. Scherpen, and D. del Puerto-Flores, "Stabilization of a class of slow–fast control systems at non-hyperbolic points," *Automatica*, vol. 99, pp. 13–21, Jan. 2019.

[28] F. Verhulst, *Methods and Applications of Singular Perturbations: Boundary Layers and Multiple Timescale Dynamics*. New York, NY, USA: Springer, 2005.

[29] D. Rimorov, I. Kamwa, and G. Joós, "Quasi-steady-state approach for analysis of frequency oscillations and damping controller design," *IEEE Trans. Power Syst.*, vol. 31, no. 4, pp. 3212–3220, Jul. 2016.

[30] J.-H. Liu and C.-C. Chu, "Long-term voltage instability detections of multiple fixed-speed induction generators in distribution networks using synchrophasors," *IEEE Trans. Smart Grid*, vol. 6, no. 4, pp. 2069–2079, Jul. 2015.
[31] S. Dehghan, N. Amjady, and A. Kazemi, "Two-stage robust generation expansion planning: A mixed integer linear programming model," *IEEE Trans. Power Syst.*, vol. 29, no. 2, pp. 584–597, Mar. 2014.
[32] X. Zhang and A. J. Conejo, "Robust transmission expansion planning representing long-and short-term uncertainty," *IEEE Trans. Power Syst.*, vol. 33, no. 2, pp. 1329–1338, Mar. 2018.
[33] S. Boyd, S. P. Boyd, and L. Vandenberghe, *Convex Optimization*. Cambridge, U.K.: Cambridge Univ. Press, 2004.
[34] K. C. Kosaraju, M. Cucuzzella, J. M. A. Scherpen, and R. Pasumarthy, "Differentiation and passivity for control of Brayton–Moser systems," *IEEE Trans. Autom. Control*, vol. 66, no. 3, pp. 1087–1101, Mar. 2021.
[35] G. H. Hardy, J. E. Littlewood, G. Pólya, G. Pólya, and D. Littlewood, *Inequalities*. Cambridge, U.K.: Cambridge Univ. Press, 1952.
[36] 2014, "Commercial and residential hourly load profiles for all TMY3 locations in the United States [data set]," National Renewable Energy Laboratory. [Online]. Available: https://ahd.csiro.au/other-data/typical-house-energy-use
[37] Z. Fu, M. Cucuzzella, C. Cenedese, W. Yu, and J. M. A. Scherpen, "A distributed control framework for the optimal operation of DC microgrids," in *Proc. IEEE 61st Conf. Decis. Control (CDC)*, Cancun, Mexico, 2022, pp. 4585–4590.
[38] S. H. Schwartz, "Normative influences on altruism," in *Advances in Experimental Social Psychology*, vol. 10. New York, NY, USA: Elsevier, 1977, pp. 221–279.

Shuai Feng (Member, IEEE) received the B.Eng. degree in mechatronics engineering from the Wuhan University of Science and Technology, Wuhan, China, in 2011, the M.Eng. degree in mechatronics engineering from Northeastern University, Shenyang, China, in 2013, and the Ph.D. degree in systems and control from the University of Groningen, Groningen, The Netherlands, in 2018. He was a Postdoctoral Researcher with the Tokyo Institute of Technology, Tokyo, Japan, in 2019, and the University of Groningen from 2020 to 2021. He is an Associate Professor with the School of Automation, Nanjing University of Science and Technology, Nanjing, China. His research interests include security of cyber–physical systems, networked control systems, and control of smart grids.

Michele Cucuzzella (Member, IEEE) received the M.Sc. degree (Hons.) in electrical engineering and the Ph.D. degree in systems and control from The University of Pavia, Pavia, Italy, in 2014 and 2018, respectively. Since 2021, he has been an Assistant Professor of Automatic Control with the University of Pavia. From 2017 to 2020, he was a Postdoctoral Fellow with the University of Groningen, The Netherlands. He has coauthored the book *Advanced and Optimization Based Sliding Mode Control: Theory and Applications* (SIAM, 2019). His research activities are mainly in the area of nonlinear control with application to the energy domain and smart systems. He received the Certificate of Outstanding Service as a Reviewer of the IEEE CONTROL SYSTEMS LETTERS 2019. He also received the 2020 IEEE TRANSACTIONS ON CONTROL SYSTEMS TECHNOLOGY Outstanding Paper Award, the IEEE Italy Section Award for the best Ph.D. thesis on New Technological Challenges in Energy and Industry, and the SIDRA Award for the best Ph.D. thesis in the field of Systems and Control Engineering. He was also a finalist for the EECI Award for the best Ph.D. thesis in Europe in the field of Control for Complex and Heterogeneous Systems, and for the IEEE-CSS Italy Best Young Paper Award. He has been serving as an Associate Editor for the EUROPEAN JOURNAL OF CONTROL since 2022 and the European Control Conference since 2018.

Thijs Bouman received the Ph.D. degree in social psychology from the University of Groningen in 2016 and has been affiliated with the Environmental Psychology Expertise Group sice 2016. He is an Assistant Professor of Environmental Psychology with the Faculty of Behavioural and Social Sciences, University of Groningen, The Netherlands. He has worked as an Advisor for the European Commission's Joint Research Center Directorate-General Energy, the Energy Academy Europe, the Dutch Health Council and the Dutch Ministry of Economic Affairs and Climate Policy. He investigates individual, social, and contextual factors that influence people's energy preferences, choices, and behaviours which affect the efficiency and sustainability of ESI. He has acquired funding from the Netherlands Organization for Scientific Research, the EU (ERA-Net and H2020), and Governments. His research has been published in key psychological, engineering and multidisciplinary research journals, such as *Nature Sustainability*, *Global Environmental Change*, *One Earth*, *Energy Research and Social Science*, and *IEEE Power and Energy Magazine*.

Linda Steg studied Adult Education with the University of Groningen. She received the Ph.D. degree from the University of Groningen in 1996. She is a Professor of Environmental Psychology with the University of Groningen. She has worked with the Netherlands Institute for Social Research, The Hague. She studies factors influencing sustainable behavior, the effects and acceptability of strategies aimed at promoting sustainable behavior, and public perceptions of technology and system changes. She is a Laureate of the Dutch Royal Decoration with appointment as the Knight of the Order of the Netherlands Lion and the Stevin prize of the Dutch Research Council. She is a lead author of the IPCC special reports on 1.5°C and AR6 published in 2018 and 2022, and participates in various interdisciplinary and international research programmes in which she collaborates with practitioners working in industry, governments, and NGOs. She is a member of the Royal Netherlands Academy of Sciences and the European Academy of Sciences and Arts.

Jacquelien M. A. Scherpen (Fellow, IEEE) received the Ph.D. degree in applied mathematics from the University of Twente, The Netherlands, in 1994. She was a Faculty with the Delft University of Technology in 2007. Since 2006, she is a Professor with the Jan C. Willems Center, ENTEG, Faculty of Science and Engineering, University of Groningen. From 2013 to 2019, she was the Scientific Director of ENTEG. She is currently the Director of the Groningen Engineering Center and the Captain of Science of the Dutch High Tech Systems and Materials Top Sector. Her research interests include model reduction for networks and nonlinear systems, modeling and control of physical systems with applications to electrical circuits, mechanical systems, and grid/network applications, including distributed optimal control. She has been an Associate Editor for the IEEE TRANSACTIONS ON AUTOMATIC CONTROL, *International Journal of Robust and Nonlinear Control* (IJRNC) and the *IMA Journal of Mathematical Control and Information*. She is in the editorial board of IJRNC. She is a Fellow of IEEE, appointed Knight in the Order of The Netherlands Lion, and received the best paper prize for the triennium 2017–2020 of Automatica in 2020. She is currently a member of the IFAC council. She is the Past-President of the European Control Association (EUCA), and EUCA-liaison for the IEEE CONTROL SYSTEMS SOCIETY.

Open Access funding provided by 'Università degli Studi di Pavia' within the CRUI CARE Agreement